Conduction in cosputtered Au-SiO_2 films

S. P. McAlister, A. D. Inglis, and P. M. Kayll*
Solid State Chemistry, Division of Chemistry, National Research Council of Canada, Ottawa, Ontario, Canada K1A 0R9
(Received 20 August 1984)

The percolation behavior and the temperature dependence of the resistivity of cosputtered Au-SiO_2 films has been studied in films ranging in thickness from 10 to 1000 nm. We find evidence for dimensional crossover effects. At low temperatures, weak-localization behavior with positive magnetoresistance is observed in samples on the metallic side of the percolation transition. On the insulator side of the transition and very close to it, the temperature dependence of the resistivity shows a crossover from $\exp(1/T^{1/4})$- to $\exp(1/T^{1/2})$-type behavior, suggesting that more than one conduction mechanism occurs.

I. INTRODUCTION

Cosputtered metal-insulator films show a percolation transition in the conductivity as the fraction (X) of metal is varied,[1] the position of the transition depending on the dimensionality (d) of the film. In random systems the transition occurs[2] at $X_c \sim 0.16$ in three dimensions (3D) and at $X_c = 0.5$ in two dimensions (2D). In metal-insulator mixtures the insulator is often amorphous, and preferential nucleation in the metal islands excludes the insulator atoms, which produces a coating of the crystalline metal grains[1] and a granular structure. This picture has been refined by Cohen *et al.*,[3] who maintain that the segregation of the metal is incomplete so that some metal remains dispersed in the insulator. As a result X_c is larger than that for a random arrangement of the two components. In nominally 3D films X_c may be 0.5—0.6.[1] When the thickness of such a film is comparable with the correlation length there is a crossover to lower dimensional behavior.[4]

One aim of our experiments was to examine the percolation properties of granular Au-SiO_2 films as the thickness was varied from values comparable with the average grain size to much larger values. We also wished to study the temperature dependence of the resistivity, particularly in the concentration region very close to the percolation transition where the conducting paths are very narrow and weak localization may occur at low temperatures.

This study follows our work on Cu-SiO_2 (Ref. 5) and Al-Si (Ref. 6). Previous studies on Au-SiO_2 include work on the resistivity,[7–12] temperature dependence of the resistivity in the SiO_2-rich region,[7–11] optical studies,[12] Hall effect,[13] and microstructure.[1,8,9,12]

Recent work on gold films includes the study of conduction noise in island films,[14] the fractal properties of such films,[15] and non-Ohmic conduction.[16] In these studies the percolation properties arise from the connectivity of the metal islands as the films are built up during deposition. This is in contrast to granular gold films which are two-phase materials and where the percolation depends on the fraction of metal. Since the resistance is primarily determined by the connectivity in the metallic matrix,[1] it is the dilution of the metal by SiO_2 that is vitally important. In the SiO_2-rich region the properties may depend more on the specific metal because the size of the metallic grains is extremely important and may vary for different metals, especially when films are thermally treated. Sputtered metal-SiO mixtures are not be confused with those with SiO_2 since the SiO disproportionates to $Si + SiO_2$, so that silicides may be formed.[17]

In the following section we discuss percolation, localization, and dimensional effects, followed by a description of the experiments in Sec. III and the structure in Sec. IV. Section V deals with the percolation aspects of the resistivity data and the temperature dependence is discussed in Sec. VI. Section VII contains our summary and conclusions.

II. PERCOLATION, LOCALIZATION, AND DIMENSIONAL EFFECTS

A classical percolation system is macroscopically inhomogeneous. There is a length scale ξ such that at distances larger than ξ the system is like the bulk material, whereas for distances smaller than ξ the behavior is like that at the threshold. As $X \to X_c$, $\xi \to \infty$, so if the system conducts at $X > X_c$, it becomes an insulator below X_c. The conductivity near X_c behaves as $\sigma \sim (X - X_c)^t$. The exponent for σ differs from that for ξ because the current only flows through part of the infinite cluster.[18,19]

In this paper we are concerned not only with the percolation behavior of our samples, but also with quantum localization,[20] which arises from microscopic disorder. Theoretical discussion of the interplay between localization and percolation has been limited.[21–23] Shapiro,[22] following Khmel'nitskii,[21] shows a "phase diagram" of the microscopic resistance versus percolation probability, for a 3D random system. We use the recursion relations of Shapiro[22] to extend the diagram from 3D to 2D for $T = 0$. This we show in Fig. 1, where the macroscopic classical disorder is represented by the metal fraction (X) axis, and the quantum disorder by the ρ axis. ρ is the resistance of an elementary scatterer, normalized to $\pi\hbar/e^2$. Thus ρ is the resistance due to disorder *within* the metallic parts of the films and is independent of X.

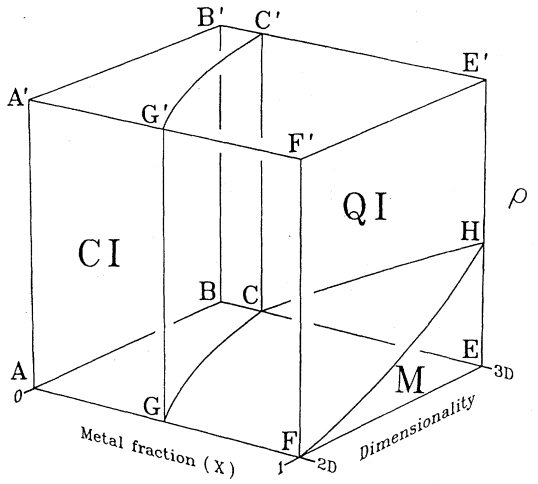

FIG. 1. Phase diagram at $T=0$ illustrating the behavior of a random system as a function of metal fraction (X) and normalized resistance (ρ) for dimensionality from 2D to 3D. The surface CC'G'G divides the classically insulating (CI) region from the rest, which is divided into metallic (M) and quantum insulating (QI) regions by the surface CGFH. The diagram follows from equations of Shapiro (Ref. 22).

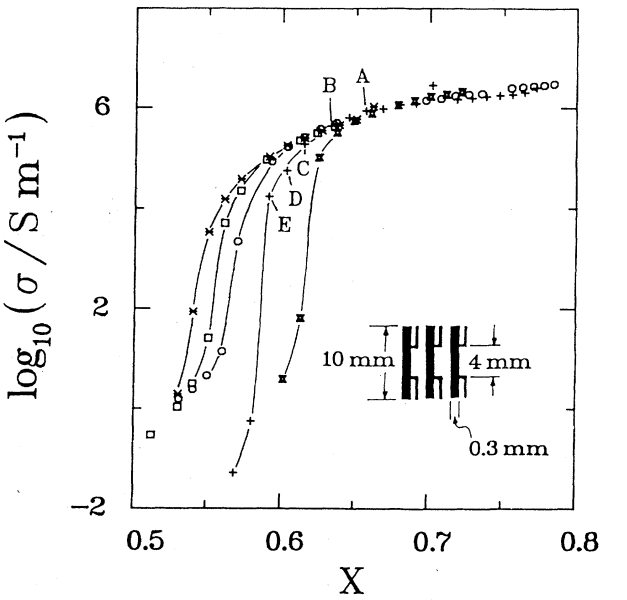

FIG. 2. Room-temperature conductivity (σ) as a function of metal fraction (X) for a range of thickness corresponding to sputtering times (in min) of 0.75 (⧓), 1 (+), 4 (○), 30 (□), and 120 (⋊). Deposition rates (nm/min) were typically 5.7 for Au and 3.6 for SiO_2. Lines are guides to the eye. Inset shows the sample shape.

In Fig. 1 the behavior of random mixtures of an ideal conductor with an insulator is represented by the base plane ABEF. Films are metallic in region CGFE and classically insulating elsewhere. The percolation threshold varies with dimensionality along the line CG. The surface CC'G'G divides the phase diagram into a classically localized region and one where there is at least one infinite cluster. In 2D all states are localized at $T=0$ and samples are insulating regardless of X. Thus only localization, classical (AA'G'G) or quantum (GG'F'F), occurs in 2D. In 3D (the plane BB'E'E) the critical flow line CH separates the classically metallic regime into metallic and quantum-localization parts. This part of the diagram has been discussed in Refs. 21 and 22. Between 3D and 2D other critical flow lines and similar X-ρ diagrams can be determined. These generate the critical surface for quantum localization CGFH, between the loci of the nontrivial fixed points represented by the lines CG and HF. These two lines are not flow lines like CH or GF. HF is a line which depicts the variation of the critical resistance for quantum localization with dimensionality, in a single-component film that has only microscopic disorder.

Although Fig. 1 represents the $T=0$ case we regard it as a qualitative illustration of the behavior of films at low temperatures as a function of dimensionality and of disorder. We may view the dimensionality axis as the variation of ξ/d or L_i/d where L_i is the inelastic scattering length and d the film thickness. For large ξ/d (or L_i/d) the film is effectively 2D, but 3D if the value is small. Figure 1 shows how the behavior can vary from metallic to weakly localized as a function of T before the classical percolation limit is reached. The figure also suggests how a series of thin films of different compositions may be represented at room temperature along a line parallel to and near the ABEF plane. At lower temperatures the line would be different, especially if the "dimension" axis is regarded as L_i/d, and the transitions then occur at different metal fractions.

III. EXPERIMENTAL DETAILS

The samples were made by rf diode sputtering with purified argon using a power level of ~0.1 kW. The target was either a composite target: a gold disk (3.8-cm diameter) mounted on a silica disk (7.5-cm diameter), or a 7.5-cm diameter split target which consisted of roughly semicircular gold and silica portions. The gold was 99.9999% pure, obtained from Cominco American Inc., Washington, and the SiO_2 was 99.99% pure, supplied by Metron Inc., New Jersey. Prior to each sputtering run the substrates were sputter-etched and the target presputtered for 30 min. The substrates were Fisher glass microscope slides cut to approximately 12×12 mm.

The sample shapes were defined by scratching the design on the film, using a metallic scribing tip in place of the pen in a high-quality plotter. This method is particularly useful when the sample dimensions are millimeters in size and particularly easy when the plotter is driven by a computer. Mask methods and photolithography proved to be far less convenient for pattern generation in our films. Typically seven four-probe samples each 0.3 mm wide were generated per slide with a separation between voltage probes of 4 mm. Typical sample shapes are

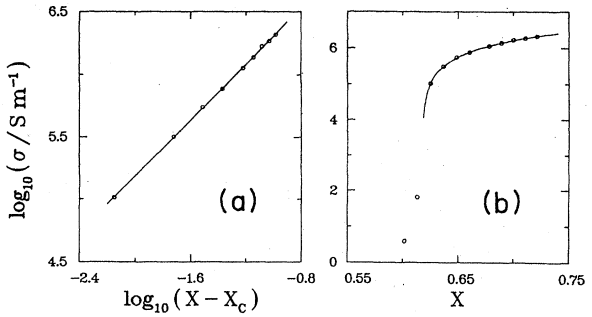

FIG. 3. (a) Log-log plot of σ at 293 K versus $X-X_c$. Line is a least-squares fit to give the conductivity exponent t and prefactor σ_0. Films were sputtered for 0.75 min. (b) Semilogarithmic plot of data from (a) compared with the fitted curve.

shown in the inset to Fig. 2. The ratio of the width of the step edge of the scribed sample to the sample width was less than 4×10^{-3}. These measurements were made with a Sloan Dektak profilometer which was used to measure sample thicknesses.

The electrical measurements were made with dc currents of mA or less depending on the sample resistance, care being taken to reduce the Ohmic heating to an absolute minimum. Contacts to the samples were made with Cu wire either ultrasonically soldered with indium or attached with silver paint, and were checked for ohmicity. The ultrasonically bonded leads were found to cycle best. For the very high-resistance samples a high-impedance electrometer (Keithley model no. 619) was used instead of a digital voltmeter (Keithley model no. 181 or Hewlett Packard model no. 3478).

The fraction of gold in the films was determined by the method of Hanak *et al.*[24] The thickness variation of the samples across the substrates was determined for the thick films and a curve fitted to this data. The same variation was assumed to be valid for all sputtering times. We assume that the thickness of the films, at any point on the substrate, varies linearly with sputtering time. This may be in error when the times are very short and nucleation of the films begins, but in this case the thickness itself is an ill-defined quantity. Since surface roughness also affects the films we have not investigated the ultrathin-film region where island growth begins.

IV. STRUCTURE

Our films have a microstructure similar to those reported for other metal-insulator films.[1] X-ray diffraction showed that the Au was crystalline with the lattice parameter of pure Au. This contrasts with Si-Al where we found the Al lattice expanded compared with the bulk.[6] X-ray linewidth measurements yielded an Au crystallite size of ~7 nm for the thin films. There is no evidence of crystalline SiO_2 in the as-deposited films—we conclude it must be amorphous. Electron micrographs were similar to those reported in the literature for other cosputtered mixtures. The metal regions were often surrounded by insulator and the films were not a random distribution of metal and insulator. In the metal-rich region the metal grains touch to form a metallic film with insulator inclusions, whereas in the dielectric region the situation is reversed.

TABLE I. Room-temperature parameters for data of Fig. 2 fitted to Eq. (1).

Sputtering time (min)	X_c (±0.002)	t (±0.03)	σ_0 (10^7 S m^{-1}) (±0.03)
0.75	0.618	1.12	2.7
1.0	0.600	0.93	1.1
4.0	0.575	1.46	2.9
30	0.554	1.88	4.6
120	0.541	2.16	6.9

It has been found by others[1] that sputtered SiO_2 is stoichiometric and does not dissociate as does SiO. We thus do not expect any Si in the film, nor any Au compounds. There may be Ar in the films but we think it relatively unimportant in our electrical studies.

V. PERCOLATION PROPERTIES

In Fig. 2 we show the way in which film conductivity σ varies with X for sets of films made using different sputtering times. The thickest films are ~1100 nm and the thinnest ~10 nm. The position of the percolation threshold varies with sample thickness, the thinnest films having the highest threshold.

Although we do not have a random percolation type of structure in our films, each of our sets of data can be fitted to

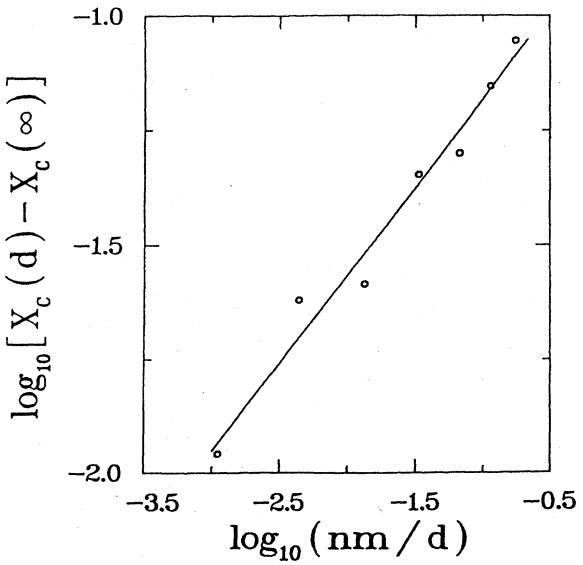

FIG. 4. Variation of the critical metal fraction (X_c) with thickness (d).

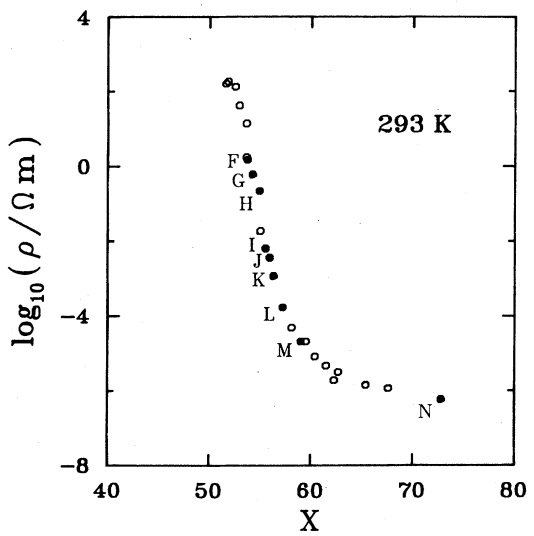

FIG. 5. Percolation behavior at 293 K of the resistivity of a series of 120-min samples. Temperature dependences of labeled samples are shown in Figs. 6, 11, and 12.

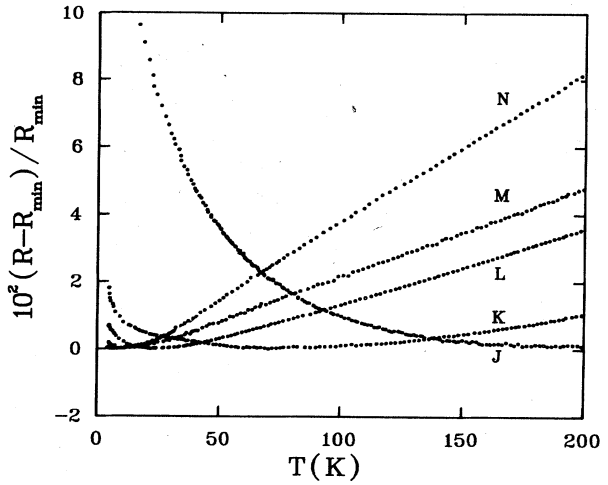

FIG. 6. Temperature dependence of the resistance (R) normalized to the minimum value (R_{min}) for a series of films referred to in Fig. 5.

$$\sigma=\sigma_0(X-X_c)^t\,, \tag{1}$$

where X_c is the metal fraction at the percolation threshold, and σ_0 and t are constants for a set of films. In the random percolation case, for which this expression was derived, the value of t varies with dimensionality being approximately 2 for 3D and 1 for 2D films (Bergman[25] gives an up-to-date table of critical exponents related to the percolation problem).

We first generated a fit to the (σ,X) experimental data, then took the value of X at maximum $\partial\sigma/\partial X$ as a first approximation for X_c. In many cases this first approximation was sufficient, in that a log-log plot of σ versus $X-X_c$ gave a straight line. Where this was not the case, a small adjustment to X_c was necessary. A least-squares fit to the log-log plot gave values of the exponent t, and σ_0. A typical $\log\sigma$ versus $\log(X-X_c)$ plot is shown in Fig. 3(a). Figure 3(b) shows a comparison between the experimental values of σ and X and the curve calculated using Eq. (1) and values of σ_0, X_c, and t determined using the procedure outlined above. It has not yet been explained satisfactorily why Eq. (1) should describe so well the behavior of nonrandom systems such as these granular films, although it is suggested[26] that it is the distribution of barrier thicknesses between grains which provides the random element.

In Table I we give values of σ_0, X_c, and t for the films of Fig. 2. Values of t vary from ~ 2 to ~ 1 as we go from our thickest to our thinnest set of films, implying a gradual crossover from 3D to 2D behavior. Random composites of conducting and insulating beads of intermediate thickness show a sudden crossover when X is varied.[4] Kapitulnik and Deutscher[27] claim to have seen a similar crossover in the behavior of Al-Ge films but we have pointed out[28] some inconsistencies in their data and interpretation. We find no evidence of a crossover of this nature in our films—intermediate thickness films yield an intermediate value of exponent t over the whole range of samples in a set, rather than different values for different regions within the set.

In Au-SiO_2 we find that X_c varies from 0.62 to 0.54 as we go from thin to thick sets of samples, consistent with previous values for similar films.[29] Kapitulnik *et al.*[30] have shown that for a random percolation system intermediate values of X_c are obtained, even for samples which are 2D according to the exponent t. They explain this as a dimensionality effect, and show that their threshold is approximately determined by the relation

$$X_c(d)=X_c(\infty)+(A/n)^{1/\nu_3}\,, \tag{2}$$

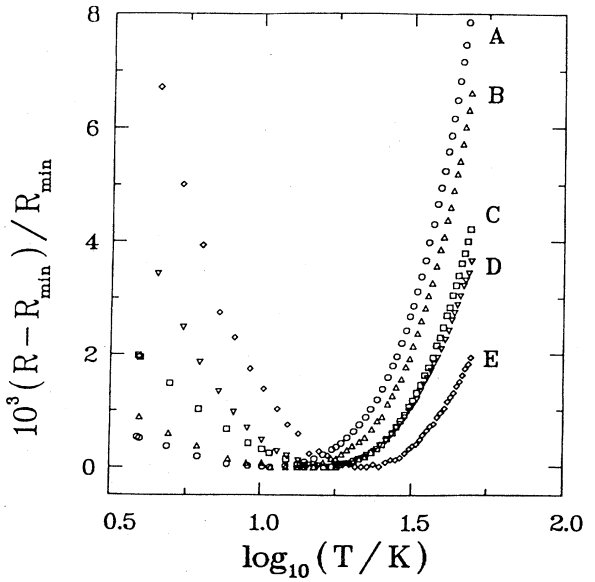

FIG. 7. Similar to Fig. 6 but for a 1-min set of samples. Temperature axis is logarithmic. Percolation behavior of the set is shown in Fig. 2.

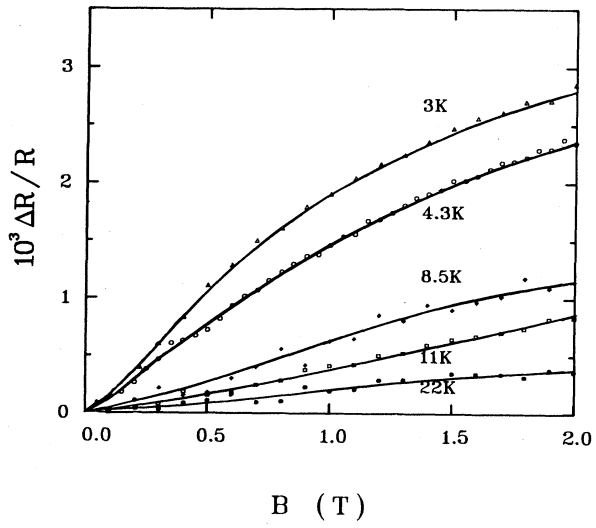

FIG. 8. Field dependence of the magnetoresistance $\Delta R/R = [R(B) - R(0)]/R(0)$ for a thin (1 min) sample at the temperatures indicated. The minimum zero-field resistance is at 13 K.

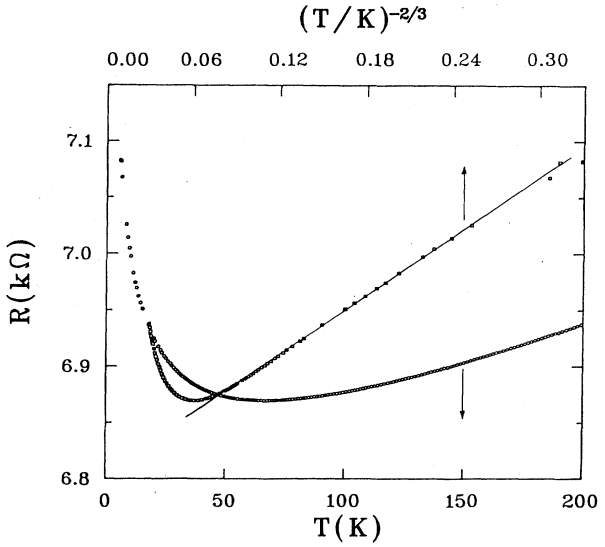

FIG. 9. Temperature dependence of the resistance of a 10-min film from the center of the transition region. Resistance is approximately proportional to $T^{-2/3}$ at low temperatures.

where $X_c(\infty)$ is the threshold value for 3D or bulk material. A is a constant, $n \sim d/a$ is the number of "layers" of material with grains of size a in a film of thickness d. The exponent ν_3 is the correlation-length exponent in 3D.

We have attempted a similar analysis for our samples. Since there is some variation in thickness across each sample set, we have used values of thickness measured or calculated as near as is possible to the same position on the substrate each time. In Fig. 4 we show $\log[X_c(d) - X_c(\infty)]$ plotted against $\log(1/d)$, where we have taken $X_c(\infty) = 0.53$. The solid line is a least-squares fit to the data, which is reasonably linear. This suggests that the shift in percolation threshold is similar to that calculated and measured for random systems, although the end points and range of values are different in the two cases. However, when we extract ν_3 and A from Fig. 4, we obtain unreasonable values ($\nu_3 = 2.6$ and $A = 8.4 \times 10^{-4}$; cf. values in the random case of 0.98 and 0.33, respectively[30]).

In summary, the conductivity of our films fits a typical percolation-theory power law [Eq. (1)] with threshold values in agreement with those found previously for granular systems. The exponent t varies with thickness suggesting a 2D to 3D crossover as a function of thickness. We find no evidence for a crossover as a function of metal fraction, as has previously been found for random composites of conducting and insulating beads.[4] While we obtain a linear behavior in the log-log plot which compares percolation threshold with film thickness [Eq. (2)], the constants which our data yield have unusual values. This suggests that the principle of the relationship as expressed in Eq. (2) is appropriate for our films but the detail is not. Further work on the theory of these granular systems is required.

VI. TEMPERATURE DEPENDENCE OF THE RESISTANCE

We have measured the temperature dependence of the resistance for a large number of films, over a range of thickness and composition. (σ versus X for a typical set at 293 K is shown in Fig. 5, the behavior of the individually labeled samples being discussed below.) The behavior, which is essentially independent of thickness, falls into three categories depending on whether the film is in the metallic, transition, or dielectric regime. In the metallic regime the resistance increases linearly with temperature above 20 K as one would expect from phonon scattering. The temperature coefficients of resistivity $(1/R)\,dR/dT$ increases with X (Fig. 6). Since the most metallic thick samples show normal metallic behavior, magnetic impurities are not a problem.

Figure 7 shows the variation with temperature of the resistance of a series of thin (1-min sputtering time) samples. (The labels refer to Fig. 2.) As in Fig. 6, we have normalized the resistance to the minimum resistance and plotted $[R(T) - R_{\min}]/R_{\min}$ versus temperature. The dominant features are the resistance minima which become more and more apparent and shift to higher temperature as the percolation threshold is approached. These observations are similar to those we made on Cu-SiO_2.[5] Since the minima become less and less apparent at large metal fractions, they cannot be caused by magnetic impurities.

For thicker films similar results are observed (Fig. 7) so these effects are not restricted to ostensibly 2D samples. However, the minima appear at metal fractions further from the threshold with the thinner samples. We believe that the observations are understandable in terms of weak localization effects. Most reported results are for thin single-component films which effectively behave as 2D

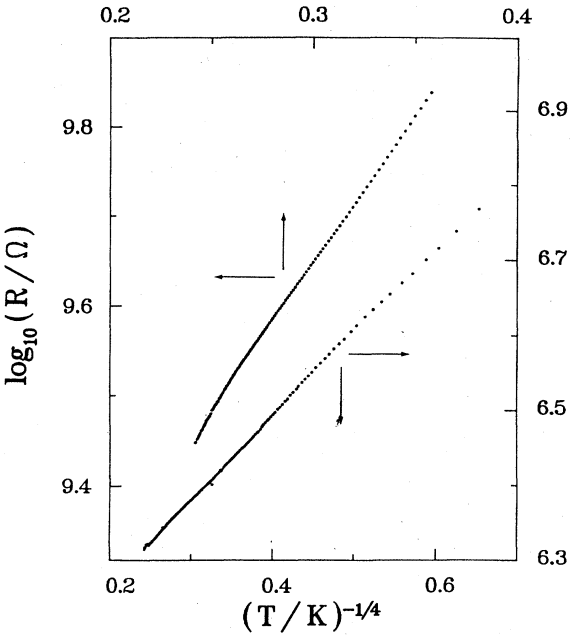

FIG. 10. Semilog plot of the resistance of two films showing approximate $\exp(T_0/T)^{1/4}$ behavior. The higher resistance sample had been sputtered for 1 min and the other for 30 min.

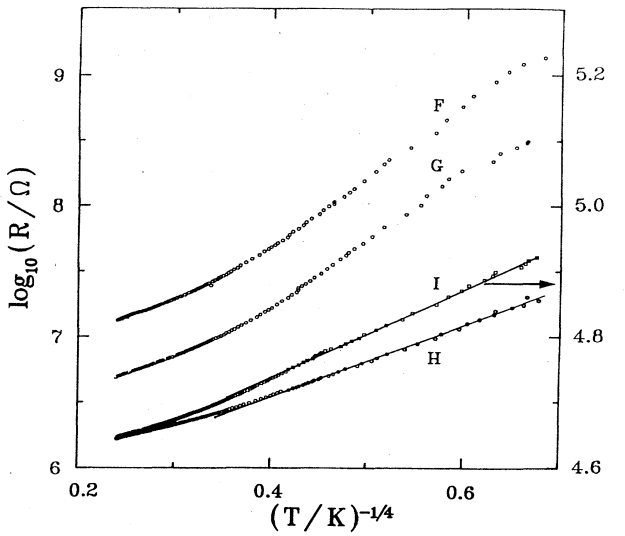

FIG. 11. Semilog plot of adjacent 120-min films plotted as a function of $T^{-1/4}$. Labels refer to samples in Fig. 5.

films at low temperatures because the inelastic scattering length is greater than the thickness. Metal-oxide-semiconductor field-effect transistors show similar 2D behavior. If the films are 2D the temperature dependence of the resistance at low temperature is $\propto \log T$. Our samples do not fit this behavior well, although we have not extended our studies to very low temperatures (fractions of 1 K). Kawaguti and Fujimori[31] have studied thin gold films at low temperatures and claim the resistance varies as $\log T$. A close examination of their data shows that there is curvature in their plot of R versus $\log T$. Clearly if one wants to distinguish $\log T$ behavior from any other dependence, one needs data over at least one decade of temperature, extending to temperatures well below the minimum.

Gold films are believed to show strong spin-orbit effects in the magnetoresistance due to localization. This manifests itself as a positive magnetoresistance.[31,32] In Fig. 8 we show the temperature dependence of the magnetoresistance for a thick granular film which had a resistance minimum at 13 K. The magnetoresistance is positive in agreement with the work on pure gold films. This is evidence that the minima are caused by weak localization effects and not magnetic impurities, since the latter would produce negative magnetoresistance.

The crossover from the weak localization to the dielectric regime, where the localization is classical, is abrupt. Adjacent samples may show completely different behavior because they are not on the same side of the threshold. It is not very easy to get samples in the range 20 to 500 $k\Omega$ because of the rapid change in resistance with X. In one case with a sample in the middle of the critical region it was very difficult to get accurate dc resistance readings. It also proved impossible to get accurate temperature-dependent data because of the excessive noise in the sample. (This current noise has been studied before in pure gold films.[14])

In Fig. 9 we show results for a film which is on the very steep portion of the R versus X curve. Here the characteristic length for percolation is most probably much larger than the thickness of the sample and also comparable to or larger than the inelastic scattering length in the Au. This produces an unexpected $1/T^{2/3}$ behavior. The sample did cycle well, so this was not a time-dependent or an annealing effect.

On the insulating side of the percolation threshold the metal grains are isolated from each other, and if they are attached to neighboring grains there is no infinite cluster. As a result conduction arises partly from the tunneling of electrons between isolated metallic grains or clusters. Within each grain there may be band conduction but this is relatively unimportant as far as the temperature dependence is concerned if the grains are large. In the dielectric regime an electron has to be removed from one neutral grain to the next, creating a pair of charged grains.[1] The process requires a charging energy since the grains have a small but finite capacitance. This energy is supplied thermally so that in weak electric fields thermally activated behavior occurs. In many cases the resistance varies as $\exp(T_0/T)^{1/2}$, which has been predicted using the charging model.[33] Simanek[34] has extended the model to consider the effect of energy-level splitting due to the finite size of the grains. Since this splitting is inversely proportional to the volume of the grains it dominates for small grains. Simanek[34] produces the $\exp(T_0/T)^{1/2}$ dependence using the approach of Refs. 35 and 36. The model has undergone further refinement by Sheng and Klafter,[37,38] referred to as KS, who suggest that the $T^{-1/2}$ dependence arises as the interpolation between low- and high-temperature behavior. KS predict that the Mott

$\exp(T_0/T)^{1/4}$ behavior should apply at low temperatures and a simple activated one at high temperatures.

An alternative theory[39] based on a reexamination of the variable-range hopping model predicts that the dc resistivity should behave as $\exp(T_0/T)^{1/2}$ at low temperatures and crossover to a $T^{-1/4}$ dependence at a temperature T_c. According to Ref. 40, T_c is so high that the crossover would be difficult to observe.

The functional dependence on temperature that is attributed to experimental data depends on the range the data is fitted over and often on the viewpoint of the observer. The quality and temperature range of the data are very important in distinguishing one law from another. Some authors who have studied Au-SiO_2 in the dielectric regime seem convinced that the resistivity obeys a simple Arrhenius law, yet the data do not justify such an interpretation. The data often require the activation energy to be temperature dependent.

In Fig. 10 we show data for two samples, one very thin and one that is far thicker, plotted logarithmically as a function of $1/T^{1/4}$. The behavior is not $\exp(1/T^{1/2})$. Both the samples in Fig. 10 are just on the dielectric side of the percolation threshold and are examples where the hopping interpretation appears to be applicable since the grains cannot be well isolated from each other.

In Figs. 11 and 12 data for four thick films are shown. Figure 11 shows $\log_{10}R$ versus $1/T^{1/4}$ and Fig. 12 $\log_{10}R$ versus $1/T^{1/2}$. The four samples in the figures were adjacent on a substrate on the dielectric side of the percolation threshold (see Fig. 5). There are regions of both plots which are approximately linear, the $1/T^{1/2}$ curve being a good description of the high-temperature region whereas $1/T^{1/4}$ fits the low-temperature region. This supports the contention by Abeles[1] that deviations from the $1/T^{1/2}$ law occur in the transition region. We believe these results show that the KS theory applies, rather than the Efros and Shklovskii[39] one and elaborate on this elsewhere.[41]

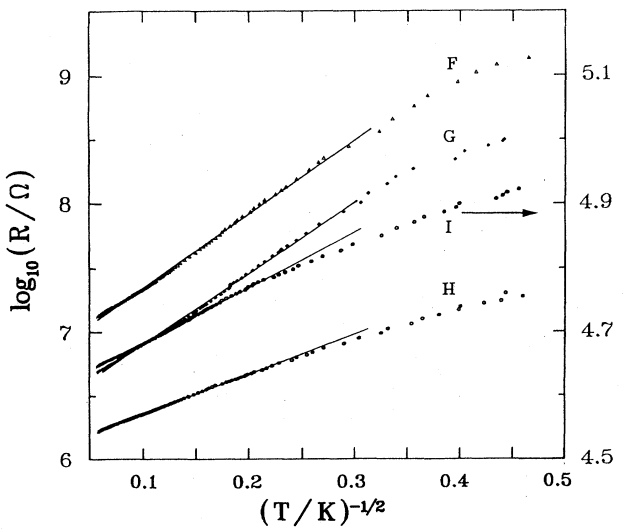

FIG. 12. Same as Fig. 11 but as a function of $T^{-1/2}$.

Transmission electron microscopy studies show that the grains are not well isolated close to the threshold, many being connected to other grains. The connections are tenuous and not necessarily metallic. We suggest that these very thin regions are sufficiently small to provide the localized states needed for variable range hopping. Larger grains, where the average diameter is larger than the very tenuous connections, will be more metallic and have very much better conductivity than the connections. The apparent breakdown of one type of behavior to another suggests that there are at least two conduction mechanisms, either of which may dominate in certain temperature ranges.

The phase diagram (Fig. 1) is for a random system at $T=0$. Our system is a granular one at finite T. Nevertheless, the observed temperature dependences of the resistance are consistent with the qualitative features of Fig. 1, although the fixed points, such as C and G are different. High X values yield samples which show weak localization only at very low temperatures, whereas samples with X values closer to X_c show evidence for it at higher temperatures. In these cases changing temperature corresponds to varying the dimensionality (through L_i/d) so we effectively pass through a surface like CGFH by lowering T. For samples extremely close to X_c the variety of behaviors seen in the temperature dependence may reflect trajectories that traverse both the quantum and classically localized regions. A separation of the quantum and classical localization effects for a particular sample is impossible because of the complicated geometrical structure of the film. The percolation behavior at room temperature, which showed gradual rather than abrupt changes in the conductivity exponent with thickness (i.e., dimensionality) is also qualitatively consistent with the phase diagram.

VII. SUMMARY AND CONCLUSIONS

We have studied percolation in Au-SiO_2 films through an electrical resistance study of films ranging in thickness from 10 to 1000 nm. They show evidence for a crossover from 3D to 2D behavior in the thickness dependence of the resistivity. We have found that, near the percolation threshold, weak localization occurs before the transition to strong, classical localization. In this regime the magnetoresistance is positive, suggesting it arises from spin-orbit coupling. Conduction via variable range hopping and tunneling between grains occurs on the dielectric side of the percolation transition, in support of the Klafter and Sheng model for conduction in granular films. The qualitative behavior of the system with variation of composition, thickness, and temperature has been found to be consistent with features contained in a phase diagram derived from ideas of Shapiro.

ACKNOWLEDGMENTS

We thank G. F. Turner for his technical assistance in preparing the films and Dr. Krishna Rajan for transmission electron microscopy work on our behalf. We are also grateful to D. R. Kroeker for making some of the measurements and Dr. J. R. Dahn for the x-ray work.

*Present address: Simon Fraser University, Burnaby, British Columbia, V5A 1S6 Canada.

[1]B. Abeles, P. Sheng, M. D. Coutts, and Y. Arie, Adv. Phys. **24**, 407 (1975); B. Abeles, *Applied Solid State Science* (Academic, New York, 1976), Vol. 6, p. 1.

[2]S. Kirkpatrick, Rev. Mod. Phys. **45**, 574 (1973).

[3]M. H. Cohen, J. Jortner, and I. Webman, Phys. Rev. B **17**, 4555 (1978).

[4]J. P. Clerc, G. Giraud, S. Alexander, and E. Guyon, Phys. Rev. B **22**, 2489 (1980); M. Rappaport and O. Entin-Wohlman, *ibid.* **27**, 6152 (1983).

[5]N. Savvides, S. P. McAlister, C. M. Hurd, and I. Shiozaki, Solid State Commun. **42**, 143 (1982); N. Savvides, S. P. McAlister, and C. M. Hurd, Can. J. Phys. **60**, 1484 (1982).

[6]A. D. Inglis, J. R. Dutcher, N. Savvides, S. P. McAlister, and C. M. Hurd, Solid State Commun. **47**, 555 (1983).

[7]N. C. Miller and G. A. Shirn, Appl. Phys. Lett. **10**, 86 (1967); in Semiconductor Products and Solid State Technology, Sept. 1967 issue, p. 28.

[8]N. C. Miller, B. Hardiman, and G. A. Shirn, J. Appl. Phys. **41**, 1850 (1970).

[9]J. K. Pollard, R. L. Bell, and G. G. Bloodworth, J. Vac. Sci. Technol. **6**, 702 (1969).

[10]T. E. Christen and J. G. Hewitt, in *Proceedings of the 1970 Electronic Components Conference* (IEEE Parts, Material, and Packaging Group) (IEEE, New York, 1970), p. 63.

[11]G. R. Witt, Thin Solid Films **13**, 109 (1972).

[12]R. W. Cohen, G. D. Cody, M. D. Coutts, and B. Abeles, Phys. Rev. B **8**, 3689 (1973).

[13]E. K. Sichel and J. I. Gittleman, Solid State Commun. **42**, 75 (1982).

[14]M. Celasco, A. Masoero, P. Mazzetti, and A. Stepanescu, Phys. Rev. B **17**, 2564 (1978).

[15]R. F. Voss, R. B. Laibowitz, and E. I. Allessandrini, Phys. Rev. Lett. **49**, 1441 (1982).

[16]G. Grimvall and T. C. Andersson, J. Phys. D **16**, 1985 (1983).

[17]C. A. Neugebauer, Thin Solid Films **6**, 443 (1970).

[18]A. Skal and B. I. Shklovskii, Fiz. Tekh. Poluprovodn. **8**, 1586 (1974) [Sov. Phys.—Semicond. **8**, 1029 (1975)]; P. G. de Gennes, J. Phys. (Paris) Lett. **37**, L1 (1976).

[19]S. Kirkpatrick, in *Electrical Transport and Optical Properties of Inhomogeneous Media,* edited by J. C. Garland and D. B. Tanner (AIP, New York, 1978), p. 99.

[20]E. Abrahams, P. W. Anderson, D. C. Licciardello, and T. V. Ramakrishnan, Phys. Rev. Lett. **42**, 673 (1979).

[21]D. E. Khmel'nitskii, Pis'ma Zh. Eksp. Teor. Fiz. **32**, 248 (1980) [JETP Lett. **32**, 229 (1980)].

[22]B. Shapiro, Phys. Rev. Lett. **48**, 823 (1982); B. Shapiro, in *Annals of the Israel Physical Society, Vol. 5: Percolation Structures and Processes,* edited by G. Deutscher, R. Zallen, and J. Adler (Israel Physical Society, Jerusalem, 1983), p. 367.

[23]Y. Gefen, D. J. Thouless, and Y. Imry, Phys. Rev. B **28**, 6677 (1983).

[24]J. J. Hanak, H. W. Lehmann, and R. K. Wehner, J. Appl. Phys. **43**, 1666 (1972).

[25]D. J. Bergman, J. Phys. A **16**, 3149 (1983).

[26]G. Deutscher, A. Kapitulnik and M. Rappaport, in *Annals of the Israel Physical Society, Vol. 5: Percolation Structures and Processes,* edited by G. Deutscher, R. Zallen, and J. Adler (Israel Physical Society, Jerusalem, 1983), p. 207.

[27]A. Kapitulnik and G. Deutscher, J. Phys. A **16**, L255 (1983).

[28]A. D. Inglis and S. P. McAlister, J. Phys. C **17**, L649 (1984).

[29]G. Deutscher, M. Rappaport, and Z. Ovadyahu, Solid State Commun. **28**, 593 (1978).

[30]A. Kapitulnik, M. Rappaport, and G. Deutscher, J. Phys. (Paris) Lett. **42**, L541 (1981).

[31]T. Kawaguti and Y. Fujimori, J. Phys. Soc. Jpn. **51**, 703 (1982).

[32]G. Bergmann, Phys. Rev. Lett. **48**, 1046 (1982).

[33]P. Sheng, B. Abeles, and Y. Arie, Phys. Rev. Lett. **31**, 44 (1973).

[34]E. Simanek, Solid State Commun. **40**, 1021 (1981).

[35]R. Kubo, J. Phys. Soc. Jpn. **17**, 975 (1962).

[36]V. Ambegaokar, B. I. Halperin, and J. S. Langer, Phys. Rev. B **4**, 2612 (1971).

[37]P. Sheng and J. Klafter, Phys. Rev. B **27**, 2583 (1983).

[38]J. Klafter and P. Sheng, J. Phys. C **17**, L93 (1984).

[39]A. L. Efros and B. I. Shklovskii, J. Phys. C **8**, L49 (1975).

[40]O. Entin-Wohlman, Y. Gefen, and Y. Shapira, J. Phys. C **16**, 1161 (1983).

[41]S. P. McAlister, A. D. Inglis, and D. R. Kroeker, J. Phys. C **17**, L751 (1984).